are unaffected by the valve reaction transients since these are internal forces.

References

[1] Stott, D., "The Design and Application of Hybrid Hydrazine Resistojets." Paper 9.3, April 1973, *Conference on Electric Propulsion of Space Vehicles,* Culham, England.

[2] Murch, C. K. and Hunter, C. R., "Electrothermal Hydrazine Thruster Development," AIAA Paper 72-451, Bethesda, Md., 1972.

[3] Barber, B. C., "A Fast Response Thrust Transducer for Gas-dynamic Thrusters," RAE TR Royal Aircraft Establishment, Farnborough, England, (in preparation).

[4] Boyd, A. H., "High Response Pulse Rocket Engine Thrust Measurement System," *Instrumentation in the Aerospace Industry,* Vol. 15, 1969, pp. 18–33; also *Proceedings of the 15th International ISA Instrumentation Symposium,*

[5] Crosswy, F. L. and Kalb, H. T., "Investigation of Dynamic Rocket Thrust Measurement Techniques," AEDC-TR-67-202, November 1967, Arnold Engineering Development Center, Tullahoma, Tenn.

[6] Crosswy, F. L. and Kalb, H. T., "Dynamic Compensation and Force Calibration Techniques for a Static and Dynamic Thrust Measurement System," AEDC-TR-68-202, Nov. 1968. Arnold Engineering Development Center, Tullahoma, Tenn.

[7] Crosswy, F. L. and Kalb, H. T., "Performance of a Dynamically Compensated Load Cell Force Measurement System," AEDC-TR-68-211, Nov. 1968, Arnold Engineering Development Center, Tullahoma, Tenn.

[8] Geffe, P. R., *Simplified Modern Filter Design,* London Iliffe Books Ltd., London, England, 1964, p. 67.

[9] Storey, D. J. and Cullyer, W. J., "Active Low-Pass Linear Phase Filters for Pulse Transmission," *Proceedings of the IEE* (Great Britain), Vol. 112, No. 4, April 1965, pp. 661–668.

[10] Gooding, F. E. J. and Good, E. F., "Active Filters—9," *Wireless World,* Vol. 76, No. 1414, April 1970, pp. 188.

AUGUST 1974 J. SPACECRAFT VOL. 11, NO. 8

Electrolytic Capacitor Power Source Design for Quasi-Steady Magnetoplasmadynamic Arcs

MARCO S. DI CAPUA* AND HELMUT L. KURTZ†
Institut für Raumfahrtantriebe, University of Stuttgart, Stuttgart, F.R. Germany

An "*LC*-Ladder" network is investigated theoretically and experimentally to determine the effect of the capacitor series resistance R_C and the inductor series resistance R_L on the shape of the current pulse, on the efficiency of energy transfer, and on the weight of the thruster system. R_C increases the risetime, decreases the duration of the constant current phase, and extends the pulse tail. The deterioration of the pulse is caused by energy dissipation within the network. A small ratio of R_C to the impedance of the network Z_o minimizes this loss. R_L causes a decay of the constant current phase and significant energy losses within the network. The number of elements in the network, multiplied by the ratio R_L to Z_o, must be small to minimize this loss. These losses imply an increased primary power source mass. However, there is a tradeoff between inductor mass (to minimize R_L) and primary power source mass.

I. Introduction

CURRENT interest in electrolytic capacitors as energy storage units for quasi-steady magnetoplasmadynamic (MPD) arcs stems from their desirable electrical characteristics which complement very closely the properties of such accelerators. The capacitor characteristics consist of their ability to store electrical charge at high capacity ($\sim 10^{-3}$ F) and low voltage (<500 v) which enables a power source composed of such units to deliver the long duration (>1 msec), high current pulses ($\sim 10^4$–10^5 amp) which are essential to the proper operation of a self-field quasi-steady MPD accelerator. In addition, electrolytic capacitors have a specific mass (~6 g/joule) which is much smaller than the mass of metallized paper (~14–35 g/joule), impregnated paper (~150 g/joule), or polycarbonate (Mylar, ~150–300 g/joule) capacitors,[1] which provides for added advantage for space applications.

Presented as Paper 73-1107 at the AIAA 10th Electric Propulsion Conference, Lake Tahoe, Nev., October 31–November 2, 1973; submitted October 30, 1973; revision received March 22, 1974. This work was sponsored by the State of Baden-Württemberg, German Federal Republic. The authors gratefully acknowledge the helpful assistance of M. Amin, M. A. Healy, E. Mangold, and H. Opperman during the course of this research.

Index categories: Electric and Advanced Space Propulsion; Plasma Dynamics and MHD; Spacecraft Electric Power Systems.

* Research Associate, currently with Physics International Company, San Leandro, Calif.

† Research Associate.

II. Electrolytic Capacitors

An electrolytic capacitor[2] consists of a metal (Al or Ta) anode plate which is coated by a thin (~1 μm) electrochemically deposited layer of oxide (Al or Ta) dielectric ($\varepsilon = 8$) which forms a semiconductor junction. The other "plate" is an electrolyte retained by a layer of porous paper. A second plate (Al or Ta) establishes contact with the electrolyte. This construction endows the capacitor with some unique properties which are summarized as follows.

a) An extremely large capacitance per unit area, due to the small thickness and large dielectric constant ε of the dielectric, which is further increased (~15 ×) by etching the anode foil. This translates directly into a large capacitance per unit weight.

b) The dielectric-metal semi-conductor junction conducts when the oxide layer is positive with respect to the coated plate. Therefore, the capacitor conducts under a voltage reversal, the uncoated plate oxidizes with a consequent loss of capacitance and gas is formed which eventually destroys the unit. The diode

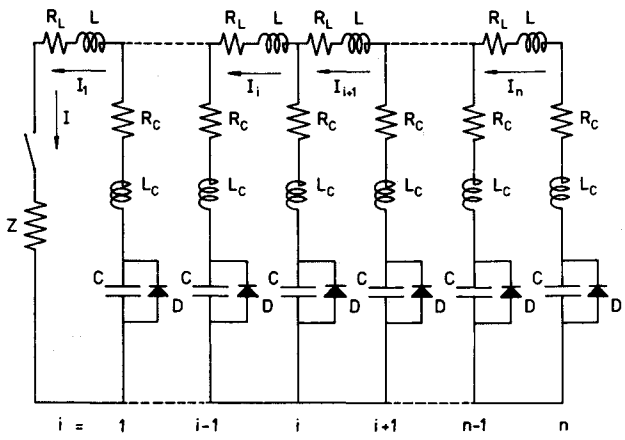

Fig. 1 "*LC*-Ladder" network schematic.

D in Fig. 1 represents this effect. Currents which would ordinarily lead to a voltage reversal must, therefore, be avoided.

c) Of the three components of the effective series resistance R_C: the resistance of the internal conductors, the resistance of the electrolyte, and the dielectric loss, the latter[2,3] is dominant.

For a lossy dielectric, R_C can be assumed proportional to its thickness and inversely proportional to its area. The converse is true for the capacitance associated with such a dielectric. Therefore, when losses in the dielectric are dominant, the product $R_C C$ is a fundamental time constant associated with a given capacitor construction. Typical values of $R_C C$ are shown in Table 1.[2,4,5]

Table 1 Typical values of $R_C C$

Capacitor type	$R_C C$ (μsec)
Polycarbonate-oil	0.2– 0.5
Oil-impregnated paper	2 – 5
Electrolytic	50 –100

Because of its small parasitic inductance L_C and large capacitance C, an electrolytic capacitor is characterized by $R_C C > 4L_C/R_C$. Under these conditions, it is well known[6] that $t_{LC} = (L_C C)^{1/2}$ determines the upper limit to the current risetime in a circuit formed by such a capacitor and $t_{RC} = R_C C$ sets an upper limit to the current and a lower limit to the duration of the current pulse which can be obtained from the capacitor. Both $(L_C C)^{1/2}$ and $R_C C$ are left unchanged by a series or parallel connection of capacitors where, for example, $R_C C = nR_C C/n$ or $R_C C = nCR_C/n$, respectively. It will be shown that these two quantities play a fundamental role in the design of a capacitive energy storage unit.

III. "*LC*-Ladder" Network Design

The task of the designer is to construct a network with nonideal circuit elements to deliver a pulse of required magnitude and duration to a load of given impedance with optimal transfer of energy and minimum weight penalty.

Among the pulse-forming networks which can be applied for this purpose, the "*LC*-Ladder" network,[7] shown schematically in Fig. 1, has been extensively used as an energy source for plasma accelerators.[1,3,5,8–14] Its salient features are as follows.

a) It consists of n shunt capacitors and n series inductors (Fig. 1) and acts ideally for $R_C = 0$ and $R_L = 0$, as a transmission line of impedance $Z_o = (L/C)^{1/2}$, and a two-way transit time $t_p = 2n(LC)^{1/2}$. The pulse has a risetime $t_c = (LC)^{1/2}$.

b) Optimum energy transfer is obtained in a single pulse when the impedance of the load $Z = Z_o$. The pulse, in this case, has a magnitude $I = V_o/2Z_o$ and a duration $t_p = 2n(LC)^{1/2}$ when the network is charged to a voltage $V = V_o$.

c) A parallel connection of m networks has an impedance $Z_o = (L/C)^{1/2}/m$, while the two-way transit time $t_p = 2n(LC)^{1/2}$ remains unchanged. On the other hand, a "series" connection of m networks has a two-way transit time $t_p = 2mn(LC)^{1/2}$ while the impedance $Z_o = (L/C)^{1/2}$ remains unchanged.

MPD arcs are, in general, low-impedance devices (10–100 mΩ). Therefore, the goal is to construct a power source of low internal impedance, taking into account the parasitic quantities R_C and L_C which will achieve optimal energy transfer. These quantities, together with the parasitic series resistance R_L of the inductors, determine the design of the network.

A straightforward design approach consists of optimizing one single network to provide a pulse of the desired shape and duration, and then utilizing a parallel connection of networks (as shown previously) to obtain the desired impedance and current level.

The first constraint to be satisfied is that both the rise-time and the fall time of the pulse must be a small fraction of the pulse length. Since $t_p = 2nt_c$, $t_c/t_p = 1/2n \ll 1$ can be satisfied by $n > 5$; by making n arbitrarily large ($\sim$20–30) and t_c correspondingly small, it would appear that pulses with a very small fractional risetime could be obtained. However, there are very severe constraints on t_c which arise as a result of the presence of R_C and L_C.

Previous calculations of Black[13] have shown that $(LC)^{1/2} > (L_C C)^{1/2}$ must be satisfied to obtain a pulse of acceptable shape ($\sim$5% ripple). Calculations, as will be shown, also indicate that minimum energy dissipation requires that $(LC)^{1/2} > R_C C$. Therefore, $(LC)^{1/2}$ must be larger than the largest of either $R_C C$ or $(L_C C)^{1/2}$. Since in most cases electrolytic capacitors are characterized by $R_C C \gg 4L_C/R_C$, then

$$(LC)^{1/2} > R_C C \gg 2(L_C C)^{1/2} \tag{1}$$

Equation (1) sets a lower limit on the transit time per station $t_c = (LC)^{1/2}$, also equal to the risetime of the pulse, which can be obtained with a given type of capacitor. This criterion is equivalent to $\beta \ll 1$ where β is defined in Eq. (3).

This minimum transit time has a simple physical explanation. The current pulse in an ideal "*LC*-Ladder" network[7] is formed by consecutive pulses of approximate duration t_c delivered sequentially by capacitors $1, 2 \ldots n-1, n, n-1, \ldots 2, 1$. Therefore, a current pulse which approximates ideal behavior can be obtained when the pulse delivered by each capacitor is shaped only by the capacitor-series inductor time constant t_c and is not choked either by the parasitic series resistance time constant t_{RC} or by the parasitic series inductance time constant t_{LC} of the capacitor.

The series resistance of the inductors R_L has a profound effect on the energy dissipation in the network and the shape of the pulse it delivers. A portion of the electrostatic energy stored in the capacitors is transferred and stored in the form of magnetic energy in the inductors before it is utilized in the load. Therefore, for minimum dissipation, a design criterion

$$t_p \gg 2L/R_L \tag{2}$$

is expected to apply as well. This criterion is equivalent to $n\alpha \ll 1$, where α is defined in Eq. (3).

IV. Network Model and Calculations

The guidelines obtained in Sec. III by simple physical reasoning, will be refined in this section utilizing numerical calculations performed on a digital computer.

The network model is shown in Fig. 1. Z, L, C, R_L, and R_C are assumed independent of frequency. The effect of L_C, exhaustively investigated by Black,[13] is not included in the calculations. Indeed, for electrolytic capacitors, the condition $t_{LC} \ll t_c$ stated in Ref. 13 is satisfied.

Kirchhoff's voltage and current relations, applied to the loops and nodes of the network with the following definitions:

$$\begin{gathered} q_i = Q_i/CV_o \qquad j_i = I_i Z_o/V_o \qquad \tau = t/t_c \\ Z_o = (L/C)^{1/2} \qquad t_c = (LC)^{1/2} \\ \alpha = R_L/Z_o \qquad \beta = R_C/Z_o \qquad \zeta = Z/Z_o \end{gathered} \tag{3}$$

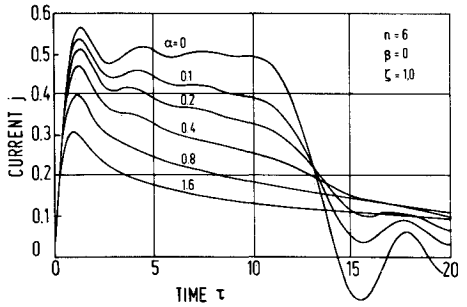

Fig. 2 Effect of inductor resistance on current waveform.

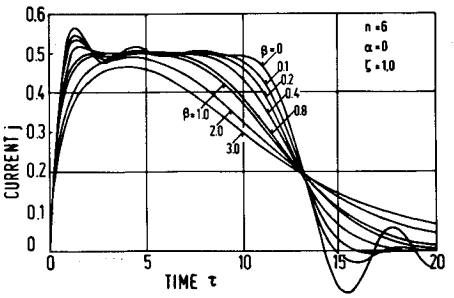

Fig. 4 Effect of capacitor series resistance on current waveform.

yield $2n$ dimensionless equations

$$\begin{aligned} dq_i/d\tau &= j_{i+1} - j_i \qquad (i = 1, n-1) \\ dq_n/d\tau &= -j_n \\ dj_1/d\tau &= -(\alpha+\beta+\zeta)j_1 + \beta j_2 + q_1 \end{aligned} \tag{4}$$

$$dj_i/d\tau = \beta j_{i-1} - (2\beta+\alpha)j_i + \beta j_{i+1} - q_{i-1} + q_i \quad (i = 2, n-1) \tag{5}$$

$$dj_n/d\tau = \beta j_{n-1} - (2\beta+\alpha)j_n - q_{n-1} + q_n$$

The dimensionless charge in capacitor i is q_i, j_i is the dimensionless current in the ith inductor, and τ is the dimensionless time. The circuit parameters as well as the initial loading voltage V_o are contained in the dimensionless variables q_i, j_i, and τ and in the dimensionless constants α, β, and ζ. The initial charge in each capacitor is CV_o; V_o/Z_o is the current delivered by an ideal network into a short circuit load; $t_c = (LC)^{1/2}$ is, as before, the transit time per station; and Z_o is the impedance of the ideal network. α, β, and ζ are the parasitic series resistance of the inductors R_L, the parasitic series resistance of the capacitors R_C and the impedance of the loads Z; all divided by the impedance of the ideal network Z_o. For example, for an ideal network discharging into a matched load ($Z = Z_o$), $\alpha = 0$, $\beta = 0$, and $\zeta = 1$.

Calculations performed by previous authors[3,7,9,14] with narrowly chosen parameters are not sufficiently broad to be used for network design. Therefore, a systematic variation of the network parameters was undertaken to determine their effect on the behavior of the network and its performance and to allow a comparison of the calculated results with experimental measurements.

Figure 2 shows the results of calculations for a 6-element network with $\beta = 0$ and $\zeta = 1$ with $\alpha = R_L/Z_o$ as a parameter. The shunt diode D is not included in the calculations. The dimensionless current j into the load is displayed as a function of the dimensionless time τ for α ranging from 0 to 1.6. For $\alpha = 0$, the ideal case, the pulse exhibits a risetime equal to 1 and a constant current $j = 0.5$ with a duration $\tau_p = 12$. The presence of α eliminates the steady portion of the pulse which for $0 < \alpha < 0.4$ is replaced by an approximately linear decay. For $\alpha > 0.4$, the decay has an exponential appearance. The maximum current is decreased since, for $\alpha > 0$, the condition $\zeta = 1$ actually corresponds to a source impedance larger than Z_o which accounts for both the lower current and a smaller energy transfer efficiency.

The efficiency of energy transfer η_α, defined as the ratio of energy delivered to the load E_z in the time τ_p divided by the energy initially stored in the network E_o, is displayed in Fig. 3. The efficiency η_α is plotted as a function of ζ with α as a parameter for the network of six elements with $\beta = 0$. The diode D is included in the circuit with an allowed voltage reversal $V_R = -0.2V_o$. The figure shows that η_α is a very sensitive function of α and that the locus of the efficiency maxima shifts from $\zeta = 1$ for $\alpha = 0$ to higher values of ζ as α increases and η_α decreases. This is understandable, since α increases the impedance of the network. Typical values of η_α are 0.9 and 0.85 for $\alpha = 0.01$ and 0.05, respectively. Because of the finite rise and fall times of the pulse, η_α does not reach unity even for $\alpha = 0$.

The dimensionless current j delivered by a 6-element network with $\alpha = 0$ into a load with $\zeta = 1$ is shown in Fig. 4 for different values of $\beta = R_C/Z_o$. The ideal network, as before, corresponds to $\beta = 0$. β dampens the oscillation during the constant current portion of the pulse and increases the risetime of the pulse. It also produces a shoulder at the trailing edge of the pulse which, when combined with the slower risetime (e.g., $\beta = 3.0$), results in the whale-shaped pulses observed by other authors.[1,14] The figure also shows, when compared to Fig. 2, that for equal values of α and β, the effect of β is much less pronounced on the shape of the pulse than the effect of α. β affects only the current delivered by each individual capacitor, while α affects a large fraction of the total current flowing in the circuit. Networks with β as high as 0.8 still produce serviceable pulses with a constant current phase whose duration is about 60% of that of an ideal network pulse.

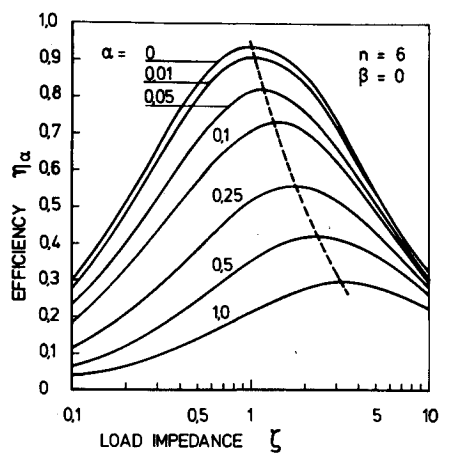

Fig. 3 Effect of relative impedance match and inductor resistance on efficiency ($\tau = \tau_p$, $\beta = 0$).

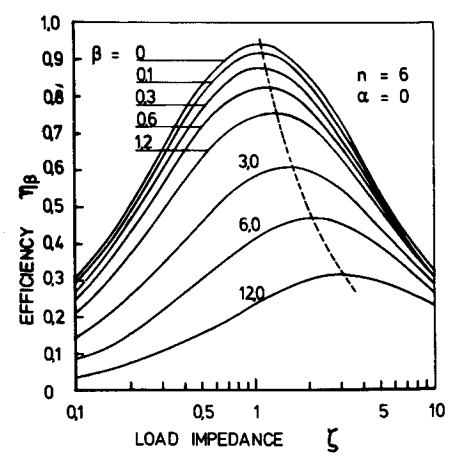

Fig. 5 Effect of relative impedance match and capacitor series resistance on efficiency ($\tau = \tau_p$, $\alpha = 0$).

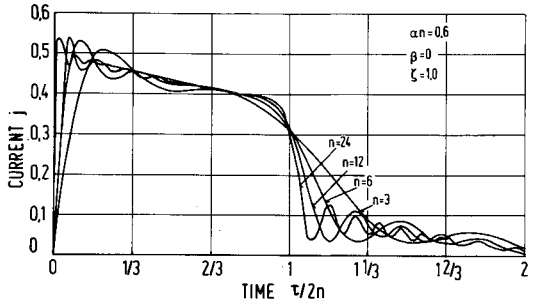

Fig. 6 Effect of number of capacitors on current waveform ($\alpha n = 0.6$).

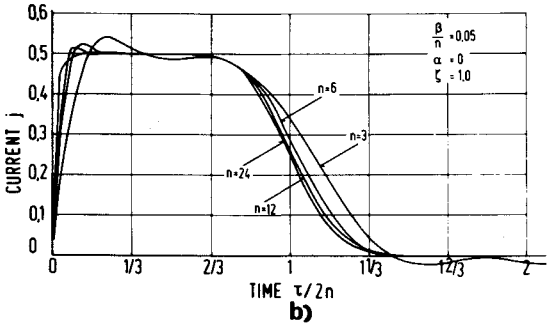

Fig. 7b Effect of number of capacitors on current waveform ($\beta/n = 0.05$).

The efficiency of energy transfer η_β is shown in Fig. 5. It is plotted as a function of ζ with β as a parameter for a 6-element network with $\alpha = 0$. The diode D is included in the calculation with $V_R = -0.2V_o$. The locus of maximum η_β shifts to higher ζ and lower η_β as β increases. Again, $\eta_\beta = 1$ cannot be achieved in $\tau = \tau_p$ for $\beta = 0$ because of the finite rise and fall time of the pulse. Wilbur[3] has indicated that results such as the ones presented in Fig. 5 remain unchanged when the parameter $\beta/n =$ constant for $5 < n < 20$. The efficiencies presented in this paper (Fig. 5) are the same as the ones shown in Ref. 3 in spite of the presence of the diode for a reverse voltage, $V_R = -0.2V_o$.‡

The conjectures presented in Sec. III were tested by performing calculations for networks of constant pulse length t_p, constant impedance Z_o, and variable number of elements. This approach allows the choice of an optimal number of elements n for a network of constant t_p and Z_o.

Calculations performed for networks of 3, 6, 12, and 24 elements are shown in Fig. 6. $n\alpha = 0.6$, $\beta = 0$, and $\zeta = 1.0$ are held constant and the time is nondimensionalized with respect to the pulse length. The risetime is inversely proportional to n as expected. The average rate of decay of the current pulse is independent of the number of elements. As the number of elements becomes large, the pulses show a striking similarity to pulses delivered into a load by a uniform transmission line (e.g., coaxial cable) with distributed resistance.[1,5] Therefore, replacing α by $n\alpha$, the pulses in Fig. 2 can be used to predict the behavior of a network with an arbitrary number of elements.

Figure 7a shows pulses for networks with $n = 3$, 6, 12 and 24 for which $\beta = 0.3$, $\alpha = 0$, and $\zeta = 1.0$ are held constant. Again, the risetime is shortened. The shoulder of the pulse, which is a feature introduced by R_C retains the same approximate shape. However, an increase of the number of elements holding β constant implies lower over-all losses (parallel connection of a large number of elements with constant resistance) and an improvement of the shape of the pulse.

A more realistic calculation is shown in Fig. 7b. The parameter $\beta/n = 0.05$ is held constant in this case. This is equivalent to the use of capacitors of constant $R_C C$ (Sec. II). Since the over-all losses are approximately constant,[3] the pulse tends to an asymptotic shape. However, the increased resistance per unit as n becomes large, causes a deformation of the leading edge of the pulse.

A step was included in the circuit equations' integration routine to prevent the capacior voltage from going below $V_R = 0$ and $V_R = -0.2V_o$ in case of a voltage reversal. The results are displayed in Fig. 8 for a network with $n = 6$, $\alpha = 0$, $\beta = 0$, and an impedance mismatch corresponding to $\zeta = 0.1$. Curve a corresponds to the ideal network (no diodes). As a result of the mismatch, the current reverses after $\tau = 13.4$ to a value which corresponds approximately to full voltage reversal. Curve b shows the effect of the diodes with $V_R = 0$. For $\tau < 12$, the pulse form is the same as for the ideal network, with a slightly higher current. For $\tau > 12$ the pulse shows a gradual drop instead of the sharp drop displayed in curve a of Fig. 8. In this case, each capacitor in the network is effectively crowbarred by the diode D. Curve c was calculated for $V_R = -0.2V_o$.‡ The pulse decay is gradual as well, but shows a steeper slope.

V. Experimental Results

Electrolytic capacitors can be successfully applied to pulse forming networks when the rules outlined in Secs. III and IV are observed. As an example, a 6-station network (Fig. 1) was assembled following such rules from electrolytic capacitors built for pulse applications.‡ The properties of the capacitors are $C = 1000\ \mu\text{F} \pm 10\%$; $R_C C = 55\ \mu\text{sec} \pm 10\%$; $(L_C C)^{1/2} = 7\ \mu\text{sec} \pm 20\%$; and $V_o = 360$ v.

These values were measured both by the small signal method[2,5] and by testing the capacitor under actual discharge conditions. The 16-turn, $L = 34\ \mu\text{H}$ and $R_L = 8.8\ \text{m}\Omega$ inductors were wound in a continuous 11.4 cm-diam, 6.35 mm-pitch solenoid with a

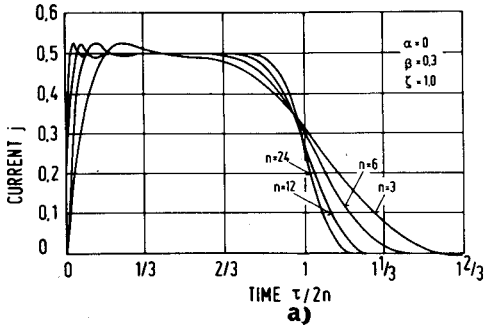

Fig. 7a Effect of number of capacitors on current waveform ($\beta = 0.3$).

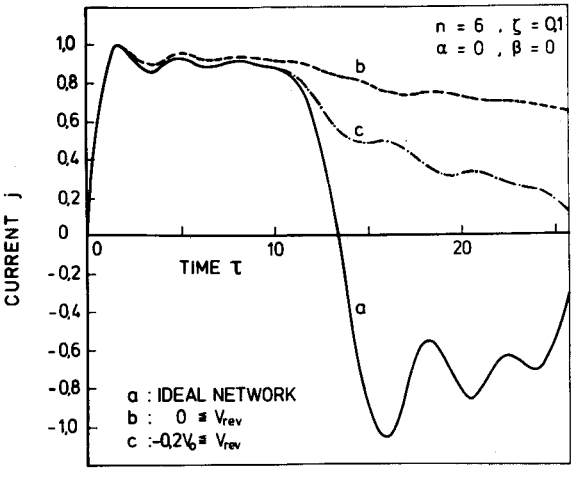

Fig. 8 Effect of shunt diode ($V_R = 0$ and $V_R = -0.2V_o$).

‡ Condenser type E 1000/360 sp, Hydrawerk AG, 1 Berlin 65, Drontheimer Straße 28–34, West Germany, 1973.

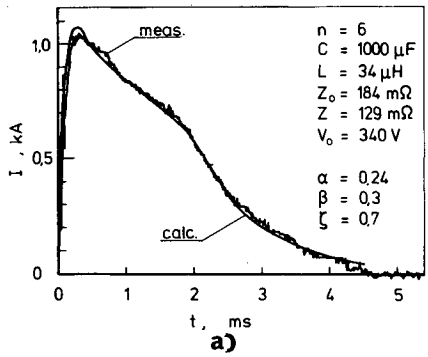

Fig. 9a Experimental and predicted current waveforms ($\alpha = 0.24$).

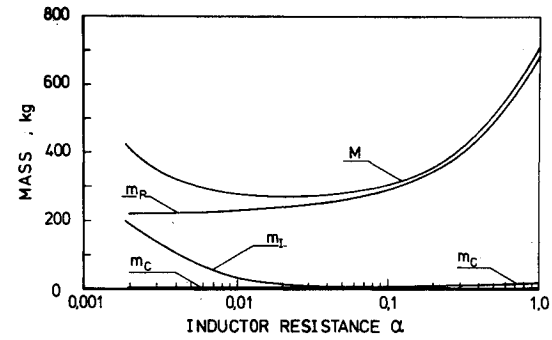

Fig. 10 MPD thruster system mass as a function of inductor resistance.

13.9 mm^2 cross-sectional area copper wire. These parameters determine $Z_o = 184$ mΩ, $t_c = 0.18$ msec, $t_p = 2.2$ msec, $\alpha = 0.048$, and $\beta = 0.3$.

Figure 9 shows the current pulses delivered by the network charged to 340 v. The current level is 1000 amp. The load is a Teflon ablation thruster with a series impendance matching resistor. The current signatures were obtained by a Rogowsky coil-passive integrator-Biomation transient recorder combination. They are displayed in the figure as the irregular traces obtained with a X-Y plotter. Figure 9a corresponds to a network whose conductor has a thinner cross section ($\alpha = 0.24$) and a load with $\zeta = 0.7$. Figure 9b corresponds to the network described above with $\alpha = 0.048$ and a load with $\zeta = 0.8$. The pulse shape arises from the effect of α and β. The former causes the steady portion to decay while the latter extends the trailing edge of the pulse. A reduction of α practically eliminates the decay of the pulse. Its steady phase, in Fig. 9b has a 1.5 msec duration. The smooth curves display the results of numerical calculations which use the measured parameters of the network and the load as imputs. Their agreement with the experimental signatures is excellent. This indicates that both the network model and calculations described in Sec. IV are correct.

A parallel connection of 16 networks presently under construction will deliver a 16.8 ka, 1.5 msec pulse, similar to the one in Fig. 9b, into a matched 12 mΩ ablation MPD thruster.

VI. Mass Considerations

Reference 3 provides some valuable mass comparisons between conventional and electrolytic capacitor pulse-forming networks without taking into account the mass of the inductors. As seen in Sec. IV, a small α optimizes both the pulse shape and the efficiency of energy transfer. This implies an increase of conductor cross-sectional area and, consequently, a higher mass for the network. The tradeoff between higher inductor and lower primary power source masses is examined in this section.

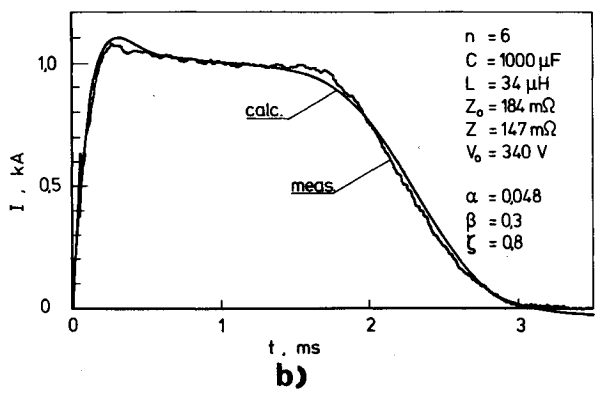

Fig. 9b Experimental and predicted current waveforms ($\alpha = 0.048$).

The mass of the inductors, assuming a solenoidal winding is

$$m_I = n\rho_w A_w(l^2 + 4\pi^2 n_I^2 r^2)^{1/2} \tag{6}$$

where n is the number of the elements of the network; ρ_w and A_w are, respectively, the density and cross-sectional area of the inductor wire; l, n_I, and r are the length, the number of turns, and the radius of the inductor section, respectively. Since

$$\alpha = R_L t_c/L = t_c(l^2 + 4\pi^2 n_I^2 r^2)^{1/2}\rho_e/A_w L \tag{7}$$

where ρ_e is the resistivity of the conductor, the mass of the inductor is

$$m_I = \rho_w \rho_e t_c(l^2 + 4\pi^2 n_I^2 r^2)/\alpha L \tag{8}$$

The total mass M of a quasi-steady MPD propulsion system operating at a constant power level P consists of the mass m_p of the primary power source (solar array + power conditioning), the mass m_c of the capacitors, and the mass m_I of the inductors. The mass of the required radiators has been neglected in Eq. (9), which gives the total mass M of the system as a function of α and β, which are included directly in the efficiency $\eta_{\alpha\beta}$

$$M = P/\gamma\eta_{\alpha\beta} + \sigma n C V_o + n\rho_e \rho_w t_c(l^2 + 4\pi^2 n_I^2 r^2)/L\alpha \tag{9}$$

where γ is the specific power of the primary power source (w/kg); σ is the specific mass of the electrolytic capacitors (kg/coul); and V_o is the charging voltage. $\eta_{\alpha\beta}$ is obtained from a plot similar to Fig. 3 calculated with the appropriate value of β.

To estimate the different terms in the equation above, a calculation was performed using typical numbers for a state-of-the-art MPD thruster system, excluding the mass of propellant and thruster head. The system mass is calculated as a function of α, assuming a pulse of fixed duration $t_p = 2.4$ msec with $n = 6$, $t_c = 2 \times 10^{-4}$ sec, $Z = 0.1$ Ω, $V_o = 350$ v, $\beta = 0.3$, and $l = 0.2$ m as a geometric constraint. The other constants are $P = 10^4$ w, $\gamma = 50$ w/kg, $\sigma = 1.3$ kg/coul^3, $\rho_e = 1.72 \times 10^{-4}$ Ωm, and $\rho_w = 8.9 \times 10^3$ kg/m^3.

Assuming an α and the above constants, $\eta_{\alpha\beta}$ and ζ are obtained from a plot similar to Fig. 3 for optimal energy transfer, following the locus of maximum $\eta_{\alpha\beta}$. Since t_c and Z are fixed, ζ determines L and l determines $n_I r$ through

$$L = \mu_o \pi n_I^2 r^2/l \tag{10}$$

M in Fig. 10 exhibits a flat minimum for α between 0.01 and 0.1 with a value of the order of 260 kg. For smaller α the mass increase is caused by the heavier inductor; for larger α it is mainly due to the steep rise of the primary power source mass required to make up the decreased energy transfer efficiencies. The share $m_c/M < 0.025$ of the electrolytic capacitors' mass is almost negligible. A reduction of R_C to zero ($\beta = 0$) would lower the total mass to some 250 kg.

VII. Summary and Conclusions

The energy dissipation caused by the series resistance of the capacitors in a pulse-forming network increases the rise-time, produces a shoulder, and extends the tail of the current pulse. The dissipation in the series resistance of the inductors, on the other hand, causes a decay of the steady phase of the pulse. Energy

dissipation is minimized when both the ratio of capacitor series resistance to network impedance and the ratio of the product of inductor series resistance times the number of elements to the impedance of the network are kept small.

The diode associated with the capacitors affects the pulse only when there is a large impedance mismatch between the network and the load. This mismatch must be avoided.

Net works constructed according to these simple rules provide excellent pulses for quasi-steady MPD accelerator operation.

The primary power source comprises the largest mass fraction of an MPD thruster system. The system mass as a function of inductor resistance exhibits a shallow minimum which arises because of a tradeoff between inductor and primary power source mass. A reduction of system mass can be accomplished by a higher specific power for the primary power source, a lower product of density and electrical conductivity of the inductor conductor, and a lower series resistance of the capacitors.

References

[1] Ducati, A. C. and Jahn, R. G., "Investigation of Pulsed Quasi-Steady MPD Arc Jet," CR 111970, 1971, NASA.

[2] *Kondensatoren 72-Handbuch,* Thomson-CSF Ltd., Munchen, West Germany, 1972.

[3] Wilbur, P. J., "Electrolytic Capacitor Pulse Networks for Quasi-Steady MPD Arcs," *AIAA Journal,* Vol. 9, No. 8, Aug. 1971, pp. 1447–1451.

[4] "Stacked Foil Compulytic ® Aluminum Electrolytics for Ultra-Low Impedance Applications," Engineering Bulletin 3443A, 1973, Sprague Electric Company, North Adams, Mass.

[5] Malliaris, A. C., John, R. R., Garrison, R. L., and Libby, D. R., "Quasi-Steady MPD Propulsion at High Power," CR-111872, 1971, NASA.

[6] Jahn, R. G., *The Physics of Electric Propulsion,* McGraw-Hill, New York, 1968.

[7] White, H. J., Gillette, P. R., and Lebacqz, J. V., "The Pulse-Forming Network," *Pulse Generators,* Vol. 5, edited by G. N. Glasoe and J. V. Lebacqz, MIT Radiation Lab. Series, McGraw-Hill, New York, 1968, Chap. 6.

[8] Posta, S. J. and Michels, C. J., "20kA PFN Capacitor Bank with Solid State Switching," *Review of Scientific Instruments,* Vol. 44, No. 10, 1973, pp. 1540–1541.

[9] Belan, N. V. et al., "Effect of Element Distribution in a Capacitor Bank on the Current Pulse in a Pulsed Plasma Injector," *Soviet Physics—Technical Physics,* Vol. 18, No. 6, 1973, pp. 749–751.

[10] Guman, W. J., "Quasi-Steady and Short Pulse Discharge Thruster Experiments," CR-111935, 1971, NASA.

[11] Ludwig, D. E. and Kelly, A. J., "Optimal Quasi-Steady Plasma Thruster System Characteristics," *Journal of Spacecraft and Rockets,* Vol. 10, No. 3, March 1973, pp. 165–169.

[12] Di Capua, M. S. and Jahn, R. G., "Energy Deposition in Parallel-Plate Plasma Accelerators," AMS Rept. 1015, 1971, Princeton University, Princeton, N.J.

[13] Black, N. A. and Jahn, R. G., "Dynamics of a Pinch Discharge Driven by a High Current Pulse-Forming Network," AMS Rept. 778, 1966, Princeton University, Princeton, N.J.

[14] Fanchiotti, A. and Simoni, G., "Alimentazione Elettrica di un Propulsore Magnetoplasmadinamico Quasi-Stazionario a Bassa Tensione," presented at the *First Congress of the AIDAA,* 1971, Palermo, Italy.

[15] Metzger, G. and Vabre, J. P., *Transmission Lines with Pulse Excitation,* Academic Press, New York, 1969.